Int J Ind Chem
DOI 10.1007/s40090-017-0114-3

RESEARCH ARTICLE

Rejection of far infrared radiation from the human body using Cu–Ni–P–Ni nanocomposite electroless plated PET fabric

Amir Khalili[1] · **Amirreza Mottaghitalab**[2] · **Mahdi Hasanzadeh**[1] · **Vahid Mottaghitalab**[1]

Received: 31 May 2015 / Accepted: 17 March 2017

Abstract An experimental investigation was utilized to present the IR rejection performance of Cu–Ni–P–Ni composite double-layer electroless plated PET fabric compared to fabric samples composed of Cu–Ni–P metallic monolayer. Accordingly, the effect of a range of operational parameters was explored on the conductivity of electroless plated PET fabric. Results indicate higher conductivity and lower durability for Cu–Ni–P-coated samples compared to its counterpart with same sub-layer included with nickel on top layer. The SEM image of Cu–Ni–P particle on PET fabric shows a hexagonal non-homogenous morphology with nanoscale crack on its surface. However, the micrograph of the Cu–Ni–P–Ni electroless plated fabric shows an extremely compact and continuous phase with clear boundaries containing semispherical particles. The thermopile radiated sensing system was used as a sophisticated device to show the thermal energy absorption level. The acquired data indicate a 2.3 and 2.7 unit reduction in transmitted radiated power, respectively, for Cu–Ni–P and Cu–Ni–P–Ni conducting fabric. The captured thermal camera images of human body while keeping in front of a Cu–Ni–P conducting fabric revealed a nearly black and blue feature which proves the significant decrease in body radiated thermal energy. However, the thermal image of Cu–Ni–P–Ni conductive fabric shows almost black appearance in all areas. It can be presumably due to improving of the IR rejection performance and also formation of a massive barrier against body thermal radiation for promising camouflage applications.

Keywords Electroless plating · Nickel · Copper · Fabric · IR rejection

Introduction

Deposition of metallic layers on fabric substrates in recent years has been area of interest for diverse applications such as electronic textiles and electromagnetic interference (EMI) shielding [1, 2]. The metalized textiles also are a preferred choice for light and radiant heat protection according to high surface reflection [3, 4]. The protection against intense radiant heat in short duration was reported for technical clothing [3]. This category of protective clothing is generally applicable for firefighter and others who exposed to high temperatures including workers in steel mills [5, 6]. Also, it can be mentioned that the metalized surface reflects solar heat during the summer and radiant heat back into the room during the winter. The textile metallization can also significantly improve the electrical conductivity and antistatic properties through conducting electricity and reducing static shock on insulated textiles [7, 8]. Moreover, the electromagnetic interference (EMI) is becoming the fourth kind of public space pollution in addition to noise, water and air pollution [1, 9]. The EMI is a well-known problem for commercial and scientific electronic instruments, antenna systems and military electronic devices. The high EMI shielding effectiveness (SE) of a typical metal is due to its high reflectance [10–12]. The previously published study indicated the high level of EMI SE of 80–90 dB for copper-plated PET fabric implying that these metallized fabrics

✉ Vahid Mottaghitalab
motaghitalab@guilan.ac.ir

[1] Textile Engineering Department, Faculty of Engineering, The University of Guilan, P. O. BOX 3756, Rasht, Guilan, Iran

[2] Chemical Engineering Faculty, Sahand University of Technology, Tabriz, Iran

Published online: 31 March 2017

can be used in the advanced electronic products and defense applications [13]. In the meantime, based on the particular specifications of the metalized textiles, promising practical potential as thermal camouflage has been reported in the literature [14, 15]. The infrared reflective materials composed of metal elements categorize in periodic table groups such as IB(Cu, Ag, Au), IIB(Zn, Cd), IIA(Be, Mg), IVA(C, Si, Ge), VIIB(Mn) and VIIIB(Fe, Ni, Co). These materials act as IR reflective layer on most substrates including textile, polymeric films and some other flexible sub-layers. In most reflection applications, it is preferred to adopt a range of total thickness between 10–50 μm and a conductive layer of 100–300 nm [16]. The clotting coated with metallic material might be a powerful reflective surface against human thermal emission detectable by thermal cameras [17, 18]. The thermal camera is a passive system working based on body reflection in middle and infrared range. Such a system works by contrasting between target IR signature and its surrounding in a wavelength range between 0.8 and 14 μm with temperature sensitivity of a few centigrade [19]. The embedded IR sensor also detects the contrast between target thermal radiation and its own background, which extremely depends on fabric optical properties. Therefore, the control of surface optical properties through morphology manipulation and conductivity adjusting plays a key role for IR rejection performance [18, 20]. In general, the contrast temperature difference is limited to 4–5 °C that needs to preserve for any atmosphere. The human skin radiates the infrared spectra in two wavelength including 32% in spectral band of 8–12 μm and 1% in spectral band of 3.3–4.8 μm. The thermal camouflage prohibits the thermal leakage but possibly creates thermal shock for wearer and reduces the overall performance. One of the main routes to remove deficiency is using the low emissivity and high reflectivity covering for prohibition of thermal radiation. The fabric finishing through lamination of a conductive layer or pattern can be a promising potential candidate in commercial bulk production. Accordingly, the variety of metalizing techniques on textile substrate was utilized to promote their properties for technical applications. The metal coating on fabric substrate is possible to be carried out using range of techniques including spraying of conductive paint [21], sputter coating [22] and electroless plating [13, 22–25]. Among the cited coating techniques, electroless plating is of special interest due to its advantages such as uniform and coherent metal deposition, good electrical conductivity and efficient heat transport. It can also be applied to almost all fiber made substances at any form of textile products such as yarn, stock, fabric or clothing. The electroless deposition method uses a catalytic redox reaction between metal ions and dissolved reduction agent [24]. For instance, the electroless copper plating is obtained through the usage of conventional sensitization and activation steps involving expensive activators such as palladium chloride (PdCl2). The great performance of Cu–Ni–P alloy electroless plated fabric on cotton fabrics makes it as an essential research area in textile finishing process. However, the oxidation process plays a disadvantageous role on conductivity and reflectivity versus time. The empirical observation reveals a significant decrease in conductivity upon exposure to atmosphere [13]. Therefore, an antioxidation layer with negligible impact on conductivity and other physical properties is extremely necessary to empower the environmental resilience of copper-coated textiles. The nickel substance is a most abundant metal potentially applicable as coating material because of its excellent corrosion and wear resistance, hardness, reflectivity and brightness [28]. Moreover, its good resistance needs to be considered against corrosion in the normal atmosphere. These properties change depending on the nickel and phosphorus levels in the deposit which in turns attributed to the composition and pH of the plating bath. The brightness and reflectivity of electroless nickel-plated surface can also significantly vary, depending on the specific formulation. The reflectivity of the deposit is also affected by the surface finishing of the substrate.

Current study focuses on the technical procedure for development of a highly durable composite conductive Cu–Ni–P–Ni layer on PET fabric by electroless plating method. The novel part of the work points out two main ideas. Firstly, the resilience promotion of previously developed material using Cu–Ni–P-coated fabric by inclusion of nickel as top layer. Then, the enhancement of thermal camouflage was highlighted using promoted technique. The fabric product after conductive finishing was characterized using scanning electron microscopy (SEM), energy-dispersive X-ray (EDX) analysis, Raman spectrometer and wide-angle X-ray diffraction (WAXD). A detailed investigation was also conducted on developed samples using thermal energy detector and thermal camera.

Materials and methods

Chemical reagents

The polyethylene terephthalate (PET) (47 × 23 Counts/cm^2, 133.7 gr/m^2, taffeta woven) fabrics with 50 cm^2 (5 × 10) surface area was used in electroless plating process. The nickel (II) sulfate hexahydrate, sodium hypophosphite monohydrate, copper (II) sulfate pentahydrate, trisodium citrate and boric acid supplied by Sigma-Aldrich and used without further purification. The

dioinized water with conductivity of less than 2 μs/cm was used in all preparation steps.

The electroless process

The electroless plating for either copper or nickel plating involves five steps including etching, sensitization, activation, electroless plating and post-treatment. Table 1 represents the composition of nickel and copper electroless bath. The whole plating procedure is illustrated schematically in Fig. 1.

The untreated fabric firstly scours and etches in 15 gr/L NaOH solution (1L) at 70 °C for 5 min prior to use and cleans with deionized water thereafter. Subsequently, the surface sensitization carries out by immersing of treated fabric samples into an aqueous solution (1 L) containing $SnCl_2$ and HCL at fixed temperature. Next, the substrate rinsed in deionized water and afterward activated by soaking in an activator solution containing $PdCl_2$ and HCL at room temperature.

The samples were then rinsed in a large volume of deionized water for more than 5 min to prevent contamination of the plating bath. Table 1 lists the composition of copper electroless bath. The pH value of the baths is adjusted by adding sufficient quantity of 10% sodium hydroxide solution. In the post-treatment stage, the plated fabrics are rinsed with deionized water at 40 °C for 20 min right after metalizing reaction of electroless plating. The prepared copper-plated fabric is immersed in the electroless nickel bath immediately to form nickel layer on

Table 1 Bath Composition and operation conditions of electroless plating

Chemical	Role	Copper electroless	Nickel electroless
Nickel(II) sulfate hexahydrate (gL^{-1})	Catalyst for copper electroless Nickel source for nickel electroless	0.25	0.75
Sodium hypophosphite monohydrate (gL^{-1})	Reducing agent	5.5	1.2
Copper(II) sulfate pentahydrate (gL^{-1})	Copper source	5.5	–
Trisodium citrate (gL^{-1})	Accelerant ligand	4	1.5
Boric acid (gL^{-1})	pH adjustor	5.5	1.2

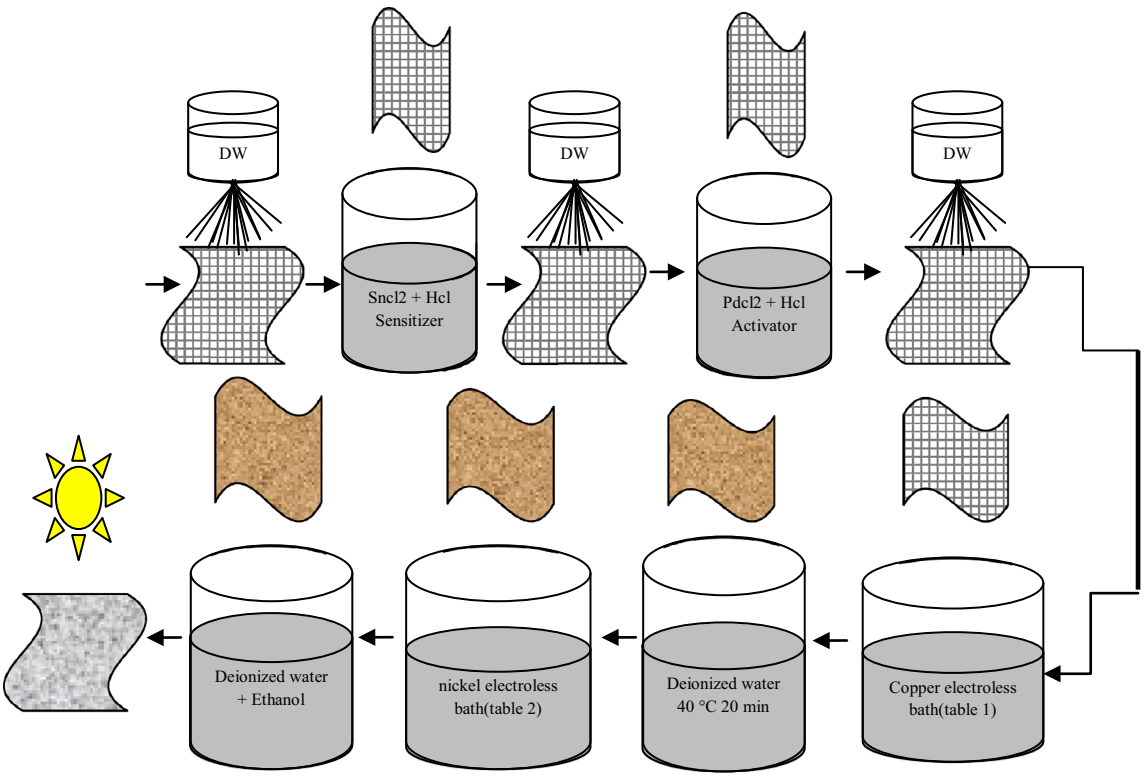

Fig. 1 Graphical representation of Cu–Ni–P–Ni plating procedure

previously copper-plated fabric. After plating, the samples are carefully rinsed with deionized water and ultimately dried in an oven at 70 °C.

The characterization techniques

The surface and cross-sectional morphologies of coated fabric were observed using Philips XL 30 scanning electron microscope (SEM). The chemical composition of plated films was determined using an elemental analysis device incorporated with SEM instrument. The crystal structure of metalized fabric before and after nickel electroless plating was also investigated using X-ray diffraction (PW1840 diffractometer, Philips) with Cu Kα radiation operating at 40 kV and 35 mA, and a scan rate of 0.1°/s. Raman spectra were characterized by Raman spectrometer (LabRam-1B, France, JY Co. Ltd). The spectra collected with a spectral resolution of 1.5 cm^{-1} in the backscattering mode, using the 632.8 nm excitation line of a Helium/Neon laser. The nominal power of the laser polarized 500:1 was 20 mW. A Gaussian/Lorentzian-fitting function was used to obtain band position and intensity. The incident laser beam was focused onto the specimen surface through a 100× microscopic objective lens, forming a laser spot of approximately 5 μm in diameter, using a capture time of 50 s. The Raman signals obtained with the half wave plate were rotated at 170° with a confocal hole set at 1100 µm and the slit set at 300 µm. The electronic balance (HR200, Japan) was used to measure the percentage of the weight change for the coated fabric compared to neat fabric. The thickness of deposits qualitatively measures by weight gain method and further confirms by metallographic cross sections of the deposits by scanning or optical microscope. The color fastness of treated fabrics was evaluated separately based on standard testing method of the ISO 105-A02:1993 (color fastness to crocking under dry and wet conditions) and ISO 105-C06:1994 (color fastness to laundering). The surface resistances of each sample were measured five times for each sample with AATCC 76-1995 standard test method. The two 2 × 3 cm^2 copper electrodes separated by 1.5 cm were placed on the each specimen and a constant 10 N force applies onto the plated fabrics. The resistance was recorded with multimeter (ADM 552R, Arma Ltd., Iran). Surface resistivity (R_s) expressed in ohms/square is calculated by equation of $R = R_s$ (l × A/w) where R is the resistance in ohms, L (cm) is the distance between electrodes, w (cm) is the width of the each electrode, and A is the fabric area in cm^2.

The transmitted thermal radiated power detects and records by utilizing a home made system using SMTIR9901 silicone infrared thermopile sensor. The SMTIR is able to detect the radiated temperature and acquired thermal power without any contact in different range of temperature. The principal specification of SMTIR9901 is a high precision and sensitivity, proper signal-to-noise ratio and response time and cutoff wavelength of 5.5 µm. The detected variation in thermal power and temperature amplifies and translates to digital value for data storage and displaying.

Microcontroller using visual basic programming employed for displaying of gathered data. Data serially transfer to main storage system to configure and record in the specific database. A general data displaying scheme employs to show the temperature, power and time data. The acquired data were categorized in a Cartesian data sheet and graph. The experiment was carried out in dark room at constant temperature of 25 °C using a standard hot surface as thermal source. Every sample fixes on hot surface for 2 min before data acquisition. The distance between thermopile sensing system and 20 × 20 cm^2 fabric sample adjusts on 10 cm. Data acquisition time and the power and temperature data can be exported in variety of spread sheet for further analysis. Every sample was experimentally tested five times to prohibit error propagation. The thermal images were captured by hot finder SAT-IR thermal camera to validate the radiated thermal power recorded by thermopile system.

Results and discussion

The mechanism of plating process

Next, following sentences focus on the mechanism of electroless copper plating of polyester fabrics that utilize the $PdCl_2$ as activator. The neat fabric substrate passes a multistep preparation procedure before soaking smoothly in copper plating bath. The concentration and temperature of activator ($Sncl_2$) and sensitizer ($PdCl_2$) baths are selected as fixed parameters based on the previously published paper regarding to copper-plated fabric [13]. Similarly, the concentration of copper electroless bath needs to be adjusted based on latest finding [13]. However, an experimental investigation conducted to find the impact of pH and temperature on average conductivity of copper-plated fabric [23, 24]. After soaking the polyester fabrics into an acidic $SnCl_2$ bath, Sn_2^+ ions adsorb onto the particle surface, forming a uniform layer. The sensitized polyester fabric then placed in the activation bath, which is prepared by dissolving $PdCl_2$ in aqueous acidic solution. This leads to the formation of Pd^{2+} ions in the activation bath, which adsorbs on the fabric surface following the addition of sensitized fabrics to the activation bath. However, Sn^{2+} ions that are present on the sensitized fabric surface immediately reduce Cu^{2+} to Cu^0. The deposited Ni^{2+} then acts as a catalyst for the subsequent Cu deposition in the

electroless plating bath. Under the catalytic action, The Ni^{2+} metallic clusters adsorb on the fabric surface. The copper ions deposit onto the catalytic nickel surface by capturing electrons that are furnished by the reducing agent [24]. In the initiation reaction, the metallic nickel clusters act as nucleation sites for copper deposition. In aqueous alkaline solutions (pH 9–10), hypophosphite as reducing agent adsorb on catalytic nickel surfaces. It is easily oxidized to yield $HCOO^-$, the activated hydrogen atom (•H) and release electrons (anodic reaction). In the meantime, the copper ions in the plating bath reduce to metallic copper by the electrons generated through the oxidation of nickel (cathodic reaction) [26]. The combination of two activated hydrogen atoms will be responsible for part of the observed gas evolution. Once the copper deposition initiates, the deposited copper atoms themselves act as self-catalysts for further copper deposition [27]. As well known, the electroless copper plating reaction represents by following chemical mechanism (Scheme 1).

Physical characteristics of Cu–Ni–P-coated fabric

The physical specifications of copper-coated fabric prepared in different pH and temperature were measured based on designated standard methods before and after color fastness tests (Table 2). According to data given in Table 2, the weight of all fabric samples increases after copper electroless plating regarding to copper formation on fabric substrate. It is evident that the higher the pH value is, the heavier the sample produces. The monotonic increase of weight continues until the pH reach to 9.5 at a fixed temperature of 70 °C (Sample 5). Similarly, the influence of temperature was also investigated at fixed pH value. The low dependence was observed for fabric weight respect to temperature change from 70 to 85 °C. In another attempt, the color fastness and corresponding electrical resistance were evaluated for fabric samples. The comparison of sample 6 and 7 shows a small difference in fabric weight before fastness test. Meanwhile, the sample 7 shows slightly smaller resistance compared to sample 6, before and after color fastness tests.

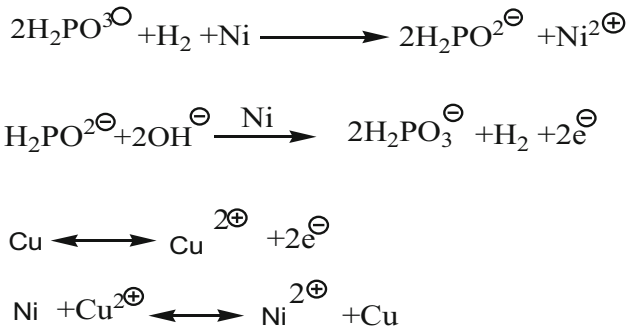

Scheme 1 Mechanism of copper electroless plating

SEM and EDAX analysis of Cu–Ni–P-coated fabric

Figure 2 shows the SEM images of PET fabric before and after electroless plating from surface of the sample 5. The acquired image in low magnification clearly reveals the presence of small particles on fabric surface. The high-resolution scanning electron microscope and EDAX analysis utilized to focus on to the coating pattern and formation process. Figure 3 clearly demonstrates the smooth and homogenous plating of copper on PET fabric. The SEM image of Cu–Ni–P particle on PET fabric shows a semi-hexagonal non-homogenous morphology with nanoscale crack on its surface. EDAX analysis and the acquired image show a compacted bulk of particles on fabric surface leads to very high conductivity for sample 5. The EDAX analysis shows copper particle and other auxiliary material. Table 3 lists the weight percent of all chemical species which were formed on fabric surfaces. Results confirm the existence of nickel particle as second top most abundant element compared to other materials. The copper reduction using sodium hypophosphate was severally investigated in previous studies [13, 23, 24, 29]. The reduction process through sodium hypophosphate is more complicated

Table 2 Effect of temperature and pH on coating weight and surface resistance before and after color fastness test

Sample	pH	*T* (°C)	Fabric weight before coating (gr)	Fabric weight after coating (gr)	Color fastness	Surface resistance (Ω/sq)	Surface resistance after crocking (Ω/sq)
1	7.5	70	0.73 ± 0.15	0.76 ± 0.13 (4.0%↑)	3	4.56 ± 0.34	12.36 ± 0.87 (171.05%↑)
2	8	70	0.7 ± 0.17	0.76 ± 0.11 (8.7%↑)	3–4	2.32 ± 0.44	4.27 ± 1.21 (84.05%↑)
3	8.5	70	0.69 ± 0.19	0.78 ± 0.15 (13.0%↑)	4	1.44 ± 0.31	2.22 ± 0.87 (54.16%↑)
4	9	70	0.72 ± 0.14	0.84 ± 0.17 (16.6%↑)	4	1.22 ± 0.54	1.87 ± 0.54 (53.27%↑)
5	9.5	70	0.72 ± 0.18	0.85 ± 0.18 (8.05%↑)	4	0.78 ± 0.15	1.28 ± 0.65 (64.10%↑)
6	9.5	75	0.74 ± 0.15	0.87 ± 0.16 (17.0%↑)	4–5	0.99 ± 0.18	1.43 ± 0.32 (44.44%↑)
7	9.5	80	0.71 ± 0.17	0.84 ± 0.14 (18.0%↑)	4–5	0.64 ± 0.14	0.92 ± 0.22 (43.75%↑)
8	9.5	85	0.72 ± 0.19	0.83 ± 0.19 (15.0%↑)	4	0.61 ± 0.18	0.97 ± 0.25 (59.01%↑)

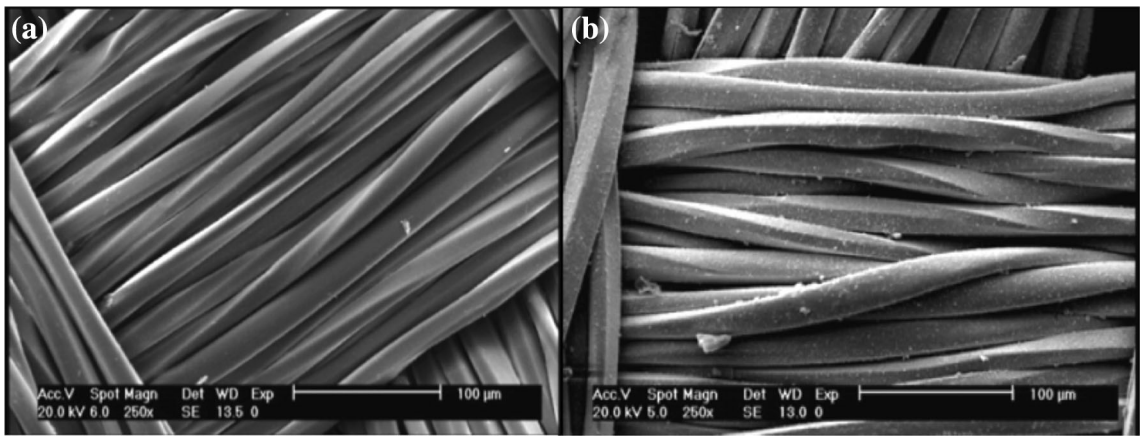

Fig. 2 SEM image of **a** the neat PET fabric, **b** Cu–Ni–P electroless plated

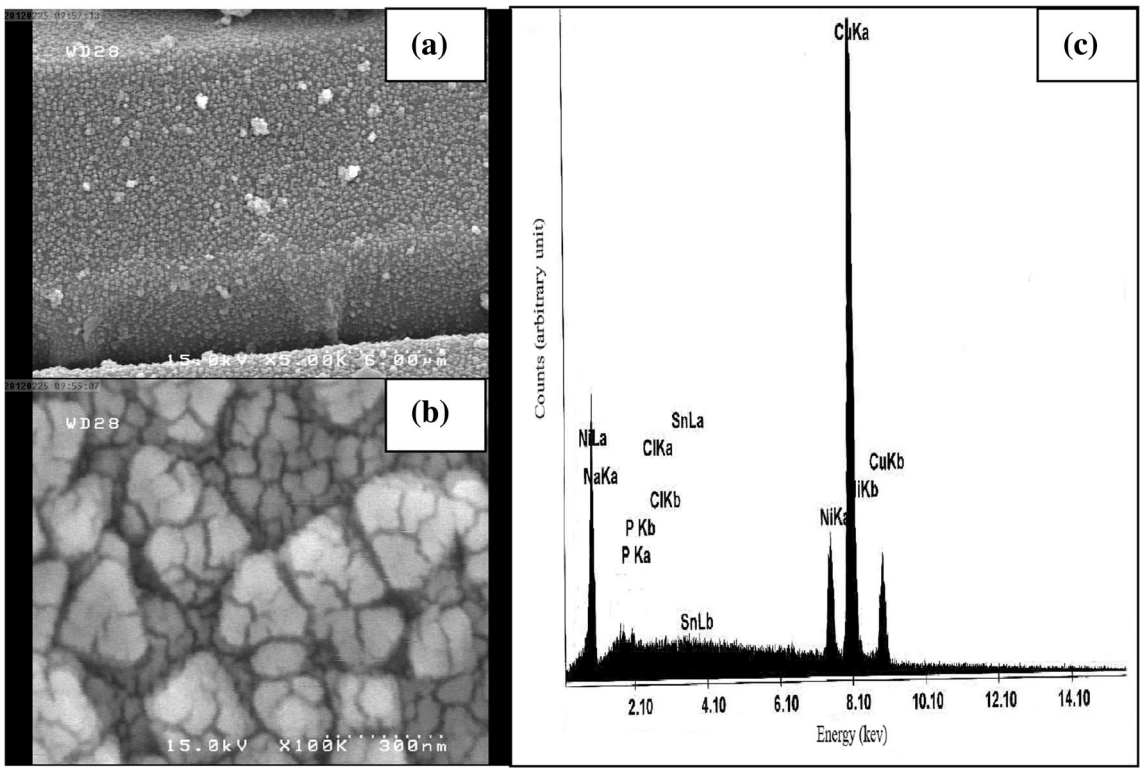

Fig. 3 SEM image of copper electroless plated **a** 5000×, **b** 10,000×, **c** the EDAX analysis of Cu–Ni–P-coated layer

compared to other process using formaldehyde as reducing agent. Since copper is not strong enough for fast oxidation of sodium hypophosphate, therefore the nickel or other metallic ion assists the oxidation process as a catalyst. Consequently, existence of nickel particle in elemental analysis of copper-plated surface is inevitable. Moreover, according to previous studies, the nickel particle assists the copper-plated fabric for being a polished surface. The reduction of copper sulfate leads to oxidizing of sodium hypophosphite using nickel sulfate, which in turn sediment nickel, and phosphorus.

The IR rejection of Cu–Ni–P-coated fabric

The IR rejection of polyester fabric coated by copper nanoparticles was characterized by thermopile sensor described in experimental section. The experiments were conducted based on the sample with high conductivity and durability, as they are most effective parameter in thermal camouflages. The detection probability of a target with a thermal imaging system is determined by the surface emissivity and temperature of the target, which is mainly controlled by the target's temperature, the radiant

Table 3 Elemental analysis of deposited particle for copper electroless plating

Element	Cu–Ni–P electroless plated	
	Atomic %	Weight %
P	1.72	0.72
Na	3.32	1.24
CI	0.07	0.04
Sn	0.19	0.36
Ni	10.04	9.62
Cu	88	84.86

waveband, direction, the target's shape and surface area. The coating process not only influences on the microstructure of fabric surface, but also changes the surface emissivity or reflectance. Since textile materials are very susceptive to IR radiation, fabric's temperature rises quickly once it is exposed to thermal sources. It is well known that the metallic-coated fabrics belong to the lower emissivity materials.

Figure 4 depicts the recorded radiated thermal power from room condition, hot source with neat fabric and hot source with copper-coated polyester fabric. The recorded data reveal a meaningful reduction in radiated thermal power detected by thermopile sensor. The experiment shows nearly constant response with little fluctuation for different sample. It can be translated as proper and reliable recording time for data acquisition. The influence of texture density on radiated power was examined by testing of neat fabric and copper-coated fabric for dense and sparsely texture fabric (Fig. 5). The sparsely texture fabric coated by copper nanoparticle shows a range of resistivity around 0.71 Ω/sq which is quite close to previous high-density sample. This leads to a 2.3 unit reduction in radiated thermal power compared to neat sparsely texture polyester fabric. However, the copper-coated dense fabric shows the lowest radiated power as it was logically expected. Figure 6 tries to explore the form and the thickness of copper

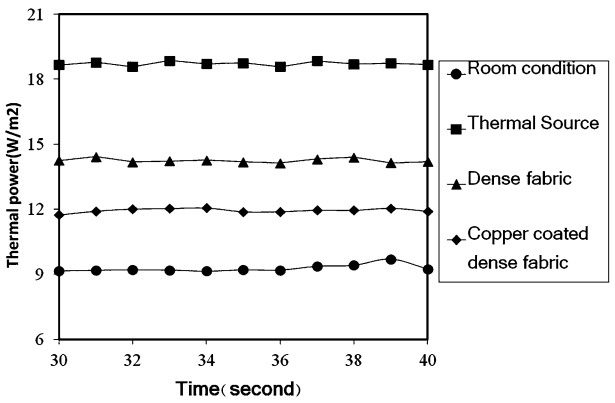

Fig. 4 Recorded thermal radiation by thermopile sensor for different condition

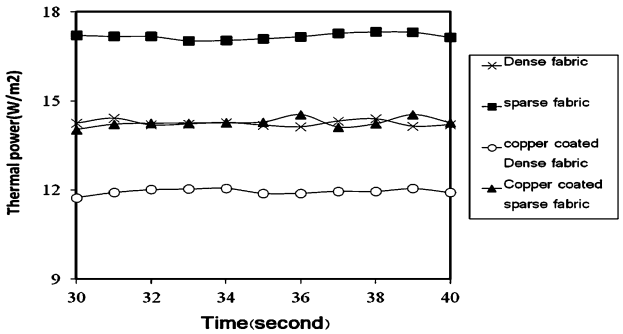

Fig. 5 Detected radiated thermal power for conductive and neat fabric with different texture

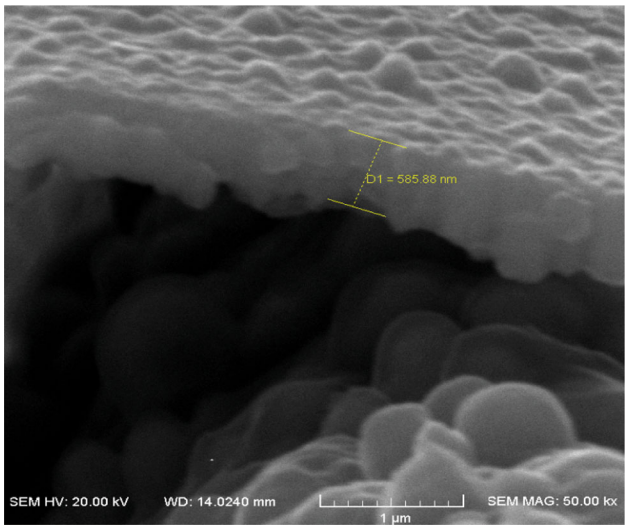

Fig. 6 SEM picture from thickness of copper deposited layer on PET fabric

layer on fabric surface. The SEM image evidences the formation of a quite smooth layer with a thickness of 585 nm. In fact, the controlling of thickness is possible based on plating duration and proposed application. The captured picture by thermal camera from a human body shows blue and black regions while keeping a piece of copper-coated dense polyester fabric (Fig. 7). The temperature indicator in right panel shows a remarkable decrease in detected temperature from 36 to 28.8 °C. This is valuable decrease in body radiated thermal energy, which locates in infrared wavelength range. There is very close coherence between conductivity data, the radiated thermal power and the thermal images. The more conductivity, the less radiation and the lower detected temperature occur. Despite very clear impact of conductive copper-coated fabric on thermal camouflage, still there is some energy leakage, which is quite evident by a narrow gap between black and blue indicating about 0.5 °C temperature difference. The first part of experiments tried to show the conductivity and its stability and homogeneity of

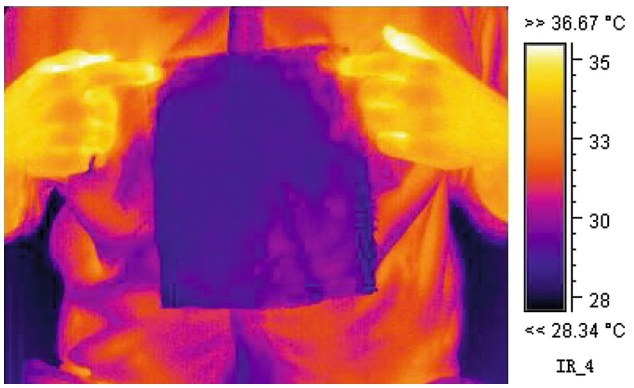

Fig. 7 Captured thermal image from human body while keeping a piece of dense copper-coated fabric

the copper-plated fabric. Results indicate the less durability due to copper oxidation for copper-plated fabric and low and non-homogenous conductivity for nickel-plated fabric because of weak coherence between particles and fabric surface. These observations are in good agreement with previously published works [13, 23, 24, 29]. Moreover, the IR- rejection of body thermal energy using copper-coated fabric shows radiation leakage which is quite enough for thermal camera detection. This problem highlights more specifically for low detection limit thermal cameras.

Physical characteristics of Cu–Ni–P–Ni-coated fabric

The rest of paper focuses on nickel coating as a top durable conductive layer on previously Cu–Ni–P composite conductive layer. Table 4 lists the electrical properties and its durability after fastness test for Cu–Ni–P–Ni nanocomposite electroless plated PET fabric as a function of temperature and pH. It can be declared that the weight of all samples significantly increases after nickel plating compared to bare copper-plated fabric. The weight measurement of other samples indicates the nickel formation on copper electroless plated fabric. Choosing suitable pH and temperature is extremely critical. In such a manner, the fabric durability after fastness test needs to be evaluated. Results exhibits most acceptable change in conductivity and its absolute value after crocking for the samples 1 and 5. However, the detailed investigation demonstrates a lower conductivity for Cu–Ni–P–Ni nanocomposite electroless plated PET fabric compared to bare Cu–Ni–P-coated fabric. It was quite predictable since the Ni presence on top surface reduces surface conductivity compared to copper particle. According to given data, the pH and temperature, respectively, adjusted on 9 and 70 °C for a nickel concentration of 1.48 gr/l.

The other strategy explains another technical procedure in order to remove deficiencies of first protocol. It can be hypothesized that the nickel lamination on top of copper-plated fabric induces both durability and homogenous high level of conductivity to fabric.

SEM and EDAX analysis of Cu–Ni–P-coated fabric

The SEM image of the nickel-plated surfaces of metallic fabric is shown in Fig. 8. It can be observed

Table 4 Effect of temperature and pH on coating weight and surface resistance before and after color fastness test for nickel-coated copper electroless plated

Sample	T (°C)	pH	Fabric weight after coating (gr)	Ni coated on copper plated	Color fastness	Surface resistance (Ω/sq)	Surface resistance after crocking (Ω/sq)
1	70	9.5	0.84 ± 0.12	0.95 ± 0.14 (13.09%↑)	4–3	1.2 ± 0.3	2.3 ± 0.4 (88.43%↑)
2	70	9	0.83 ± 0.15	0.9 ± 0.12 (8.43%↑)	3	6.3 ± 0.5	13.2 ± 2.1 (109.49%↑)
3	70	10	0.85 ± 0.17	0.96 ± 0.17 (12.94%↑)	4–3	4.2 ± 0.8	7.6 ± 1.4 (78.92%↑)
4	75	9.5	0.81 ± 0.18	0.89 ± 0.11 (9.87%↑)	4	3.5 ± 0.9	5.8 ± 2.1 (66.19%↑)
5	80	9.5	0.84 ± 0.11	0.93 ± 0.13 (10.71%↑)	4–3	2.4 ± 0.2	4.6 ± 1.1 (89.3%↑)

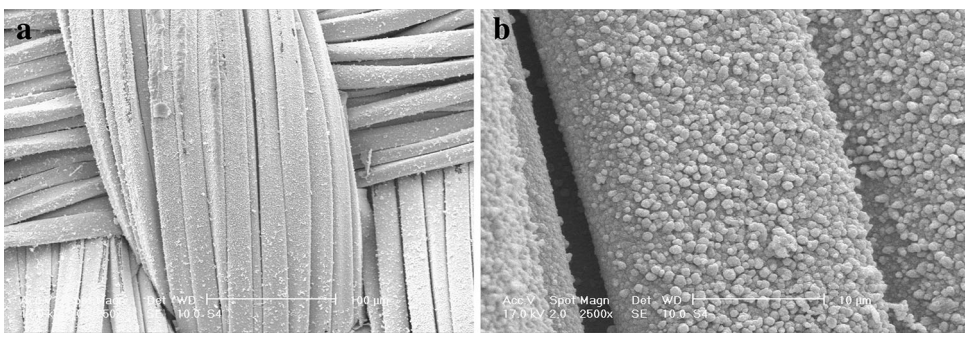

Fig. 8 SEM image of **a** Nickel plating on copper electroless plated fabric at low magnification (×500), **b** the quasi spherical nickel particle morphology at higher magnification (×2500)

that the surfaces were covered with the dense particles and evenness layers. The compactness and exceptional coherence of particles in nanoscale lead to high electrical conductivity for Ni–Cu electroless plated fabric. Figure 9 shows the particle formation and its deposited area on fabric surface in high magnification. Figure 9a apparently shows an area covered by huge numbers of nucleated particle in nanoscale range between 100 and 500 nm. The metallic fabrics were subjected to elemental analysis by EDAX analysis, and the results are shown in Fig. 9c. EDAX studies revealed that the nickel-plated metallic fabric contained mainly of copper and nickel with small amounts of tin, chlorine, sodium and phosphorus. Table 5 shows the chemical composition of metallic coatings before and after nickel electroless plating. The results show that the percentage of copper and nickel in the deposited layer, respectively, decreases and increases after nickel coating on the copper-plated fabric. On the other hand, the nickel content increases up to a certain level of the coating. The presence of nickel substance in electroless copper plating plays a key role in formation of copper layers on the fabric surface [26]. After nickel plating on the copper-plated fabric, the nickel percentage increases from 9.62 to 26.73% (% w/w). On the other hand, the copper content decreases down to a certain percent, but it has highest value within other elements.

Table 5 Elemental analysis of Cu–Ni–P–Ni plated fabric

Element	Atomic percent (%)	Weight percent (%)
P	2.63	0.81
Na	2.17	0.82
Cl	0.21	0.12
Sn	0.11	0.21
Ni	27.67	26.73
Cu	68.21	71.31

The IR rejection of Cu–Ni–P–Ni-coated fabric

Similar to first part of paper, the performance of conductive fabric is characterized by the level of deduction in transmitted power detects by thermopile sensor (Fig. 10). The Cu–Ni–P–Ni-coated fabric shows more homogenous surface compared to Cu–Ni–P-coated fabric. In addition, a thin layer around 300 nm containing nickel particle forms on previously deposited copper layer (Fig. 11). So, the Ni content is not the only reason for the IR rejection as it was tabulated in Tables 3 and 5.

The higher capability for IR ejection in Cu–Ni–P–Ni-coated fabric compared to Cu–Ni–P counterpart is a direct outcome of surface morphology. To illuminate the role of conductivity, a fabric sample with quite same range of

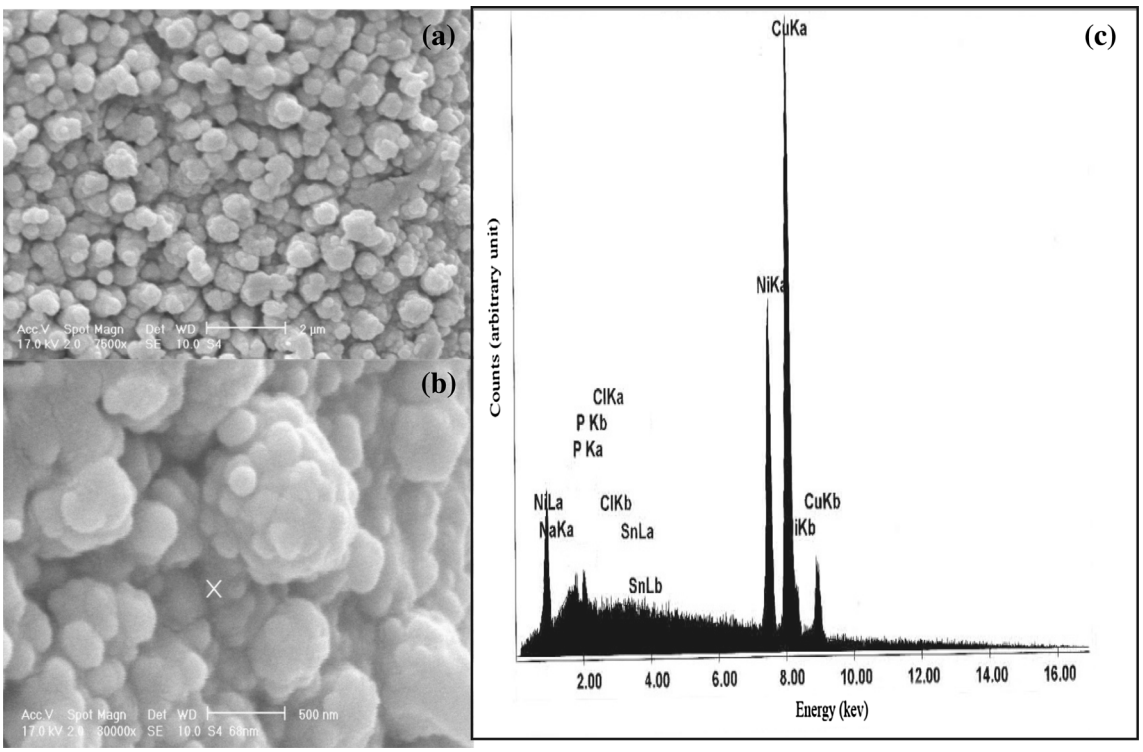

Fig. 9 SEM image of Cu–Ni–P–Ni electroless plated PET fabric **a** ×7500, **b** ×80,000, **c** the EDAX analysis of Cu–Ni–P–Ni-coated layer

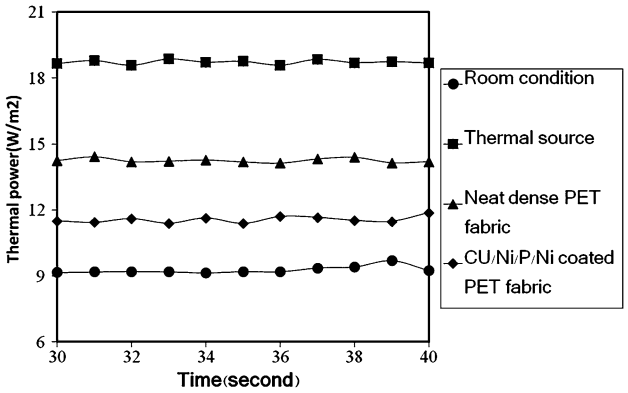

Fig. 10 Recorded thermal radiation by thermopile sensor for different condition

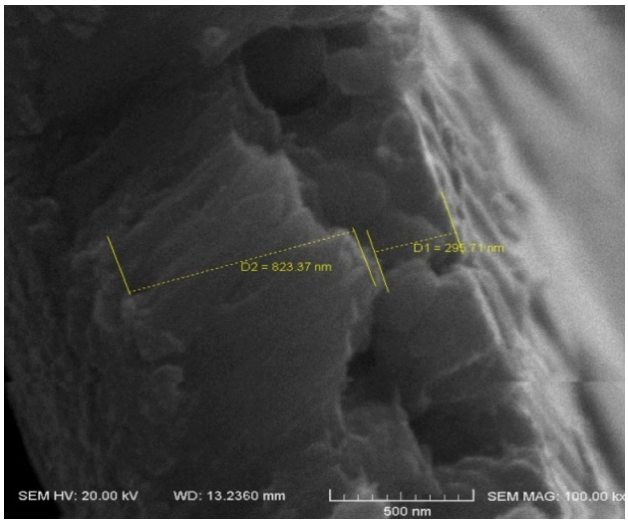

Fig. 11 SEM picture from thickness of nickel deposited layer on copper deposited PET fabric

conductivity was characterized for detection of thermal power radiation. The thermopile sensor for Cu–Ni–P–Ni-coated fabric shows a 2.7 unit deduction compared to neat fabric. The Cu–Ni–P–Ni-coated fabric shows a higher amount of rejection about 0.4 units compared to the Cu–Ni–P. The radiation leakage in first protocol can be attributed to surface inconsistency, which is probably removes by inclusion of nickel crystals. In fact, the formation of spherical particles may improves the IR rejection performance and block most of body thermal radiation. The captured thermal image reveals nearly black appearance in most areas compared to Fig. 6, which shows a black and blue color (Fig. 12). The results indicate a significant decrease in detected temperature from 36 to 28 °C. It is pronounced as efficient blockage of leaking nodes through the fabric texture after conductive finishing.

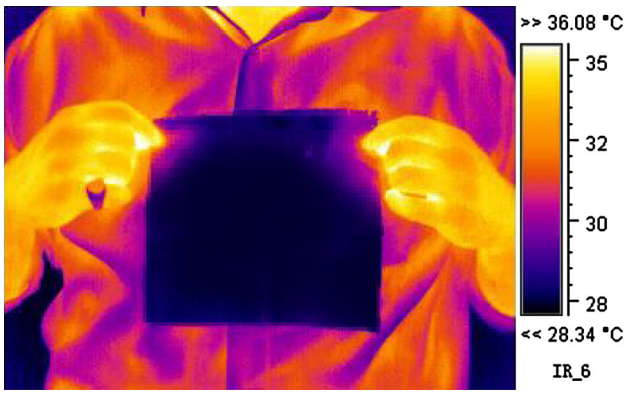

Fig. 12 Captured thermal image from human body while keeping a piece of dense Cu–Ni–P–Ni composite nanoparticle-coated fabric

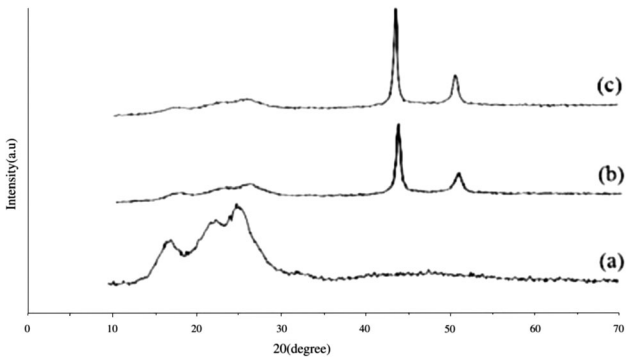

Fig. 13 XRD spectra of metallic fabrics: **a** untreated PET fabric, **b** Cu–Ni–P fabric I (1 1 1) = 13.13, I (2 0 0) = 4.75, **c** Cu–Ni–P–Ni fabric I (1 1 1) = 17.16, I (2 0 0) = 6.33

XRD and Raman analysis

Figure 13 shows the XRD patterns for metallic-coated fabrics before and after nickel plating. The strong diffraction peaks at $2\theta = 17.5°$, 22.8°, 25.3° are characteristic peaks of untreated polyester fabrics. Comparing XRD patterns shown in Fig. 13a–c, the characteristic peak intensity of the plated PET substrate is decreased obviously. As a result, the covering degree of metallic coating is compact. The XRD patterns of copper-plated PET fabric and nickel–plated metallic fabric in Fig. 13b, c were superimposed as well as the peaks that appeared at $2\theta = 43.4°$ and 50.6° and correspond to (1 1 1), (2 0 0) crystal planes, respectively. The relative intensities of the diffraction peaks from the (1 1 1) and (2 0 0) planes are listed in Fig. 13. It can be seen that the crystalline structure of the copper coating was intensified with nickel plating on the copper surface of fabric.

Raman spectra of untreated PET fabric are shown in Fig. 14a. A strong peak at 347 cm^{-1} is attributed to aliphatic chains (C–C) stretching vibration, and C–O–C

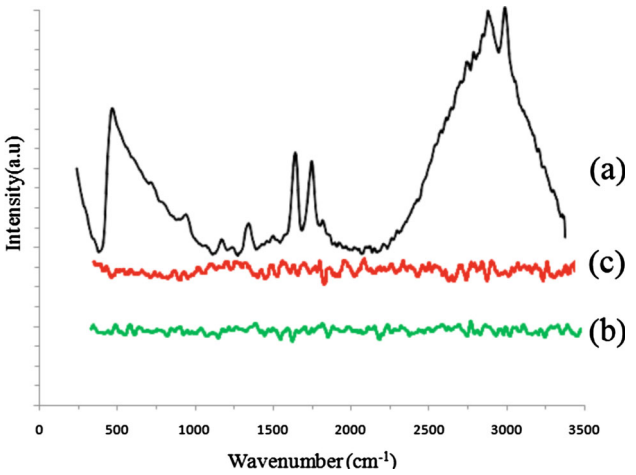

Fig. 14 Raman spectra of **a** untreated PET fabric, **b** Cu–Ni–P-coated fabric, **c** Cu–Ni–P–Ni composite nanoparticle-coated fabric

asymmetric stretching vibration is revealed at 1107 cm^{-1}. A peak at 1179 cm^{-1} belongs to ester (C(O)–O) stretching vibration. The aromatic >C=C< stretching vibration is observed at 1294 cm^{-1}. A weak peak in 1466 cm^{-1} is ascribed to the C–H stretching vibration of methylene group. Two strong peaks in 1620 and 1734 cm^{-1} are characters of phenyl ring stretching vibration and carbonyl (C=O) stretching vibration, respectively. The successive peaks in region between 2800 and 3000 cm^{-1} contribute to alkanes (C–H) stretching vibration. The alkenes (=C–H) stretching vibration developed at 3080 cm^{-1}.

Raman spectra of copper plating PET fabric and nickel-plating metallic fabrics are shown in Fig. 14b, c. Also, it can be seen that the intensity of Raman for copper-plated fabric increased after nickel plating. It can be seen that all characteristic peaks of PET fabrics are covered after metal plating. This indicates that the existence of metallic layer on the fabric surface causes a decrease in the scattering intensity by the reflection or blocking of Raman [24].

Conclusions

The high-performance conductive durable fabric was developed for rejection of emitted radiated power from thermal source in the range of far infrared similar to body thermal energy. The electroless plating of PET fabric through Cu–Ni–P formulation leads to acceptable level of conductivity and moderate durability. The specific morphology provides a medium level of blocking layer against transmitted thermal wave. It was confirmed by both thermopile sensor and thermal camera. The fur electroless nickel plating on previously surface of Cu–Ni–P PET fabric was investigated. The properties of Cu–Ni–P–Ni fabric were enhanced with respect to SEM analysis due to semispherical compact nanoparticle morphology, but there was a moderate decrease in the electrical conductivity. The nickel-coated copper-plated samples showed better properties and stable structure with uniformly distributed nickel particles. EDX shows that the chemical composition of coating still consisted mainly of copper even after nickel-plating copper-plated fabric. XRD patterns of copper-plated fabric shows that the peaks appear in the same place after nickel plating but the peaks intensity increase. Raman spectra indicate that peaks for untreated PET fabric are disappeared after plating with copper. Compared to copper-plated fabric, the Cu–Ni–P–Ni conductive fabric shows enhanced performance in terms of rejection of thermal radiation and also significant decrease in detected temperature by thermal camera.

Acknowledgements The Authors would like to express sincere appreciation from University of Guilan, Guilan Science and Technology Park (GSTP) and Iran nanotechnology initiative for their financial and technical supports.

References

1. Chen H-C, Lee K-C, Lin J-H (2004) Electromagnetic and electrostatic shielding properties of co-weaving-knitting fabrics reinforced composites. Compos A Appl Sci Manuf 35:1249–1256
2. Narasimman P, Pushpavanam M, Periasamy VM (2011) Synthesis, characterization and comparison of sediment electro-codeposited nickel–micro and nano SiC composites. Appl Surf Sci 258:590–598
3. Granqvist CG (2007) Transparent conductors as solar energy materials: a panoramic review. Sol Energy Mater Sol Cells 91:1529–1598
4. Han EG, Kim EA, Oh KW (2001) Electromagnetic interference shielding effectiveness of electroless Cu-plated PET fabrics. Synth Met 123:469–476
5. Chung G-S, Lee DH (2005) A study on comfort of protective clothing. In: Yutaka T, Tadakatsu O (eds) Elsevier Ergonomics Book Series, Elsevier
6. Raimundo AM, Figueiredo AR (2009) Personal protective clothing and safety of firefighters near a high intensity fire front. Fire Saf J 44:514–521
7. Knittel D, Schollmeyer E (2009) Electrically high-conductive textiles. Synth Met 159:1433–1437
8. Textor T, Mahltig B (2010) A sol–gel based surface treatment for preparation of water repellent antistatic textiles. Appl Surf Sci 256:1668–1674
9. Cheng KB, Ramakrishna S, Lee KC (2000) Electromagnetic shielding effectiveness of copper/glass fiber knitted fabric reinforced polypropylene composites. Compos A Appl Sci Manuf 31:1039–1045

10. Huang C-Y, Wu C-C (2000) The EMI shielding effectiveness of PC/ABS/nickel-coated-carbon-fibre composites. Eur Polym J 36:2729–2737
11. Kim MS, Kim HK, Byun SW, Jeong SH, Hong YK, Joo JS, Song KT, Kim JK, Lee CJ, Lee JY (2002) PET fabric/polypyrrole composite with high electrical conductivity for EMI shielding. Synth Met 126:233–239
12. Lee H-C, Kim J-Y, Noh C-H, Song KY, Cho S-H (2006) Selective metal pattern formation and its EMI shielding efficiency. Appl Surf Sci 252:2665–2672
13. Afzali A, Mottaghitalab V, Motlagh MS, Haghi AK (2010) The electroless plating of Cu–Ni–P alloy onto cotton fabrics. Korean J Chem Eng 27:1145–1149
14. Singh S, Suhag N (2015) Camouflage textiles. Int J Enhanc Res Sci Technol Eng 4:351–359
15. Marin N, Buszka J (2013) In: Alternate Light Source Imaging: Forensic Photography Techniques (Forensic Studies for Criminal Justice).1st edn, Anderson Publishing Ltd., Boston
16. Li Y, Wu D-X, Hu J-Y, Wang S-X (2007) Novel infrared radiation properties of cotton fabric coated with nano Zn/ZnO particles. Colloids Surf A 300:140–144
17. Wang T, He J, Zhou J, Ding X, Zhao J, Wu S, Guo Y (2010) Electromagnetic wave absorption and infrared camouflage of ordered mesoporous carbon–alumina nanocomposites. Microporous Mesoporous Mater 134:58–64
18. Yin X, Chen Q, Pan N (2013) A study and a design criterion for multilayer-structure in perspiration based infrared camouflage. Exp Therm Fluid Sci 46:211–220
19. Boukhanouf R, Haddad A, North MT, Buffone C (2006) Experimental investigation of a flat plate heat pipe performance using IR thermal imaging camera. Appl Therm Eng 26:2148–2156
20. Yin X, Chen Q, Pan N (2012) Feasibility of perspiration based infrared Camouflage. Appl Therm Eng 36:32–38
21. Azim SS, Satheesh A, Ramu KK, Ramu S, Venkatachari G (2006) Studies on graphite based conductive paint coatings. Prog Org Coat 55:1–4
22. Yip J, Jiang S, Wong C (2009) Characterization of metallic textiles deposited by magnetron sputtering and traditional metallic treatments. Surf Coat Technol 204:380–385
23. Baskaran I, Narayanan TSNS, Stephen A (2006) Effect of accelerators and stabilizers on the formation and characteristics of electroless Ni–P deposits. Mater Chem Phys 99:117–126
24. Gan X, Wu Y, Liu L, Shen B, Hu W (2008) Electroless plating of Cu–Ni–P alloy on PET fabrics and effect of plating parameters on the properties of conductive fabrics. J Alloy Compd 455:308–313
25. Lien W-F, Huang P-C, Tseng S-C, Cheng C-H, Lai S-M, Liaw W-C (2012) Electroless silver plating on tetraethoxy silane-bridged fiber glass. Appl Surf Sci 258:2246–2254
26. Gan X, Wu Y, Liu L, Shen B, Hu W (2007) Electroless copper plating on PET fabrics using hypophosphite as reducing agent. Surf Coat Technol 201:7018–7023
27. Lu Y (2009) Electroless copper plating on 3-mercaptopropyltriethoxysilane modified PET fabric challenged by ultrasonic washing. Appl Surf Sci 255:8430–8434
28. DiBari GA (1995) Nickel plating. Met Finish 93:259–279
29. Choi Y-S, Yoo Y-H, Kim J-G, Kim S-H (2006) A comparison of the corrosion resistance of Cu–Ni–stainless steel multilayers used for EMI shielding. Surf Coat Technol 201:3775–3782